AMERICAN SOCIETY FOR MICROBIOLOGY | Journal of Virology

Virology | Full-Length Text

Hypoxia and HIF-1α promote lytic *de novo* KSHV infection

See-Chi Lee,[1] Nenavath Gopal Naik,[1] Dóra Tombácz,[2] Gábor Gulyás,[2] Balázs Kakuk,[2] Zsolt Boldogkői,[2] Kevin Hall,[1] Bernadett Papp,[1,3,4,5,6] Steeve Boulant,[7] Zsolt Toth[1,3,4]

AUTHOR AFFILIATIONS See affiliation list on p. 16.

ABSTRACT The impact of different stress conditions on the oncogenic Kaposi's sarcoma-associated herpesvirus (KSHV) primary infection that can occur *in vivo* remains largely unknown. We hypothesized that KSHV can establish a latency or lytic cycle following *de novo* infection, depending on the conditions of the cellular environment. Previous studies showed that hypoxia is a natural stress condition that promotes lytic reactivation and contributes to KSHV pathogenesis, but its effect on *de novo* KSHV infection is unknown. To test the effect of hypoxia on KSHV infection, we infected cells under normoxia and hypoxia, performed a comparative analysis of viral gene expression and viral replication, and tested chromatinization of the KSHV genome during infection. We found that hypoxia induces viral lytic gene expression and viral replication following *de novo* infection in several biologically relevant cell types, in which the virus normally establishes latency under normoxia. We also found that hypoxia reduces the level of repressive heterochromatin and promotes the formation of a transcriptionally permissive chromatin on the incoming viral DNA during infection. We demonstrate that silencing hypoxia-inducible factor-1α (HIF-1α) during hypoxia abrogates lytic KSHV infection, while the overexpression of HIF-1α under normoxia is sufficient to drive lytic KSHV infection. Also, we determined that the DNA-binding domain and the N-terminal but not the C-terminal transactivation domain of HIF-1α are required for HIF-1α-induced lytic gene expression. Altogether, our data indicate that HIF-1α accumulation, which can be induced by hypoxia, prevents the establishment of latency and promotes lytic KSHV infection following primary infection.

IMPORTANCE The current view is that the default pathway of Kaposi's sarcoma-associated herpesvirus (KSHV) infection is the establishment of latency, which is a prerequisite for lifelong infection and viral oncogenesis. This view about KSHV infection is supported by the observations that KSHV latently infects most of the cell lines cultured *in vitro* in the absence of any environmental stresses that may occur *in vivo*. The goal of this study was to determine the effect of hypoxia, a natural stress stimulus, on primary KSHV infection. Our data indicate that hypoxia promotes euchromatin formation on the KSHV genome following infection and supports lytic *de novo* KSHV infection. We also discovered that hypoxia-inducible factor-1α is required and sufficient for allowing lytic KSHV infection. Based on our results, we propose that hypoxia promotes lytic *de novo* infection in cells that otherwise support latent infection under normoxia; that is, the environmental conditions can determine the outcome of KSHV primary infection.

KEYWORDS Kaposi's sarcoma-associated herpesvirus, hypoxia, lytic gene expression, primary infection, lytic cycle

Kaposi's sarcoma-associated herpesvirus (KSHV) is the etiological agent of Kaposi's sarcoma (KS) and several lymphoproliferative diseases such as primary effusion lymphoma and multicentric Castleman's disease, and it can also cause KSHV-associated inflammatory cytokine syndrome (1–3). Following primary infection, KSHV can establish

Editor Jae U. Jung, Lerner Research Institute, Cleveland Clinic, Cleveland, Ohio, USA

Address correspondence to Zsolt Toth, ztoth@dental.ufl.edu.

The authors declare no conflict of interest.

See the funding table on p. 16.

Received 1 July 2023
Accepted 12 October 2023

Published 1 November 2023

a persistent and latent infection in many different cell types *in vivo* (e.g., B cells and endothelial cells), which is characterized by the inhibition of lytic gene expression and virus production. In contrast, the lytic cycle of KSHV, which is initiated and driven by the viral replication and transcription activator (RTA), supports lytic gene expression, viral DNA replication, and virus production (4, 5). In the lytic phase, the viral lytic genes are expressed in temporal order as immediate-early (IE), early (E), and late (L) genes (6). Establishment of viral latency following primary infection is particularly important for KSHV pathogenesis, as it is a prerequisite for both lifelong infection and the development of KSHV-associated cancers (7).

The current view that the default pathway of KSHV infection is the establishment of latency is supported by the observations that KSHV latently infects most of the cultured cell lines *in vitro* (8). However, it is important to note that *in vitro* KSHV infections are usually performed under ideal cell culture conditions that are devoid of the many possible stress stimuli that can occur *in vivo* during KSHV infection. For example, it is known that the oxygen level varies significantly in different parts of the body (1%–19%), and in many cases, tissues function in a hypoxic microenvironment (<5%) (9, 10). Thus, we aimed in this study to investigate whether hypoxic stress, which is a natural inducer of KSHV lytic reactivation (11–13), can allow lytic *de novo* infection in cells that otherwise KSHV latently infects under normal or stress-free conditions.

Hypoxia changes the expression of hundreds of hypoxia-responsive genes by activating the cellular transcription factors called hypoxia-inducible factors (HIFs), which promote the survival of cells under hypoxia (14, 15). HIFs consist of either HIF-1α or HIF-2α and HIF-1β/ARNT subunits (16). During normoxia (21% O_2 level), HIF-1α is hydroxylated by a prolyl hydroxylase (PHD) at its proline residues 402 and 564. The hydroxylated HIF-1α is recognized by an E3 ubiquitin ligase complex composed of von Hippel-Lindau protein acting as the substrate recognition unit, Cullin-2, Elongin-1, Elongin-2, and RBX1, which polyubiquitinates HIF-1α at several lysine residues, resulting in its proteasomal degradation (17–19). When the cells are exposed to hypoxia, PHDs get inactivated, resulting in the stabilization of HIF-1α, which then heterodimerizes with the constitutively expressed HIF-1β in the nucleus. Upon dimerization, HIF-1α/HIF-1β binds to E-box-like hypoxia response elements (HREs) located in the promoters of hypoxia-inducible genes and upregulates their expression (20).

Hypoxia has been shown to have a pro- or anti-viral effect depending on the virus and the condition of the viral infection (21). Previous studies have demonstrated that hypoxia can induce lytic reactivation of KSHV in latently infected cells and contribute to KSHV-induced oncogenesis (12, 22). It was demonstrated that several KSHV gene promoters, including those of RTA, contain HREs; thereby, HIF-1α can activate viral gene promoters, facilitating lytic replication (23, 24). While hypoxia-induced lytic reactivation has been studied by several research groups, the effect of hypoxia on primary KSHV infection is still unknown. In this study, we have discovered that hypoxia supports the KSHV lytic cycle following *de novo* infection in various cell types. We demonstrate that HIF-1α is required for hypoxia-induced lytic KSHV infection and that HIF-1α expression alone is sufficient to support lytic KSHV infection under normoxia. Based on our results, we propose that hypoxia allows KSHV-lytic *de novo* infection in cells that otherwise support latent infection under normoxia.

MATERIALS AND METHODS

Cell lines and KSHV infection

HEK293T (ATCC), EA.hy926 (ATCC), and SLK (NIH AIDS Reagent Program) cells were maintained in Dulbecco's modified Eagle's medium (DMEM) supplemented with 10% fetal bovine serum (FBS) and penicillin-streptomycin. HULEC-5a (ATCC) and HMEC-1 (ATCC) endothelial cells were cultured in MCDB131 medium containing 10 ng/mL epidermal growth factor (ThermoFisher), 1 µg/mL hydrocortisone (Sigma), 10 mM glutamine (ATCC), and 10% FBS. TIME endothelial cells (ATCC) were cultured in Vascular

Cell Basal Medium (ATCC) supplemented with Microvascular Endothelial Cell Growth Kit-VEGF (ATCC) and 12.5 µg/mL blasticidine. KSHV [wild type (WT) and RTA knockout (KO)] was produced from iSLK-BAC16 cell lines (25). KSHV infection was performed as described previously (26). For KSHV infection of $CoCl_2$-treated cells, the cells were first treated with 250 µM $CoCl_2$ for 16 h, followed by KSHV infection, which was performed by spinoculation. The $CoCl_2$ was left on the cells during the KSHV infection. For KSHV infection under hypoxia, the cells were grown in a hypoxia incubator (1% O_2) for 16 h, then KSHV in cell culture medium was added to the cells and incubated under hypoxia. The cell culture media were changed at 8 hpi, and the cells were harvested at the indicated time points.

Antibodies

The following primary antibodies were used in the study: anti-HIF-1α (Cell Signaling 36169S), anti-ORF45 (Santa Cruz sc-53883), anti-K8.1 (Santa Cruz sc-65446), anti-FLAG (Sigma F1804), anti-Tubulin (Sigma T5326), anti-GAPDH (Proteintech), anti-H3 (Abcam ab1791), anti-H3K4me3 (Active Motif 39159), anti-H3K27me3 (Active Motif 39155), and anti-ORF6 (gift from Gary S. Hayward, Johns Hopkins University).

Immunofluorescence assay

Immunofluorescence analysis was performed as described previously (27). Briefly, SLK cells were treated with 250 µM $CoCl_2$ for 16 h, followed by KSHV infection for 40 h. Then, the cells were washed with phosphate-buffered saline (PBS), fixed with 4% paraformaldehyde for 10 min at room temperature, and then permeabilized with 0.5% Triton X-100 for 5 min. The samples were incubated in blocking buffer (10% FBS, 0.2% Tween 20, 0.2% Fish Skin gelatin in PBS) for 30 min at 37°C. Primary antibodies (ORF45 and HIF-1α) were diluted in blocking buffer at a 1:400 dilution. Primary antibody staining was performed for 1 h. This was followed by 30 min of incubation with secondary antibodies (1:400 dilution) at room temperature and then washing with PBS.

Supernatant transfer assay

SLK cells were incubated in a hypoxia incubator (1% O_2) for 16 h, followed by KSHV infection for 72 h. Supernatants were collected and filtered with a 0.45-µm SFCA syringe filter. Supernatants were supplemented with fresh medium and used to infect fresh SLK cells. After 24 hpi, infected cells were harvested, and total DNA was prepared for quantitative PCR (qPCR) analysis to determine the level of intracellular viral DNA. Based on a standard curve using KSHV BAC16 DNA and the level of intracellular DNA in the infected cells, we calculated the number of infectious viral particles in the medium used for the infection.

Nanopore sequencing

SLK cells were incubated in a hypoxia incubator (1% O_2) for 16 h, followed by KSHV infection for 72 h. Total RNA was extracted using the NucleoSpin RNA Mini kit (Macherey-Nagel). Enrichment of polyadenylated RNAs from total RNA samples was carried out using the Poly(A) RNA Selection Kit V1.5 (Lexogen). For library preparation, PolyA(+) RNAs were applied for the generation of the sequencing libraries using the Direct cDNA Sequencing Kit (SQK-DCS109), following the instructions of Oxford Nanopore Technologies. The cDNA libraries from normoxia and hypoxia samples were loaded separately onto ONT R9.4.1 SpotON Flow Cells (200 fmol mixture of libraries per flow cell). AMPure XP beads were used after each enzymatic step. Samples were eluted in UltraPure nuclease-free water (Invitrogen). Guppy basecaller (v6.3.8) was applied for analyzing the sequencing data. High-quality reads (quality filter >8) were used for mapping. Minimap2 mapper v2.17 was used for aligning the reads to the reference KSHV genome (GQ994935.1) according to the following: *-ax splice -Y -C5 -t4 -- cs*. Downstream data analysis was carried out within the R environment as published before (28). In the case of

multi-mapped reads, the alignment with the highest mapping quality was kept, and the reads were counted once. Viral genes were counted from the alignments by analyzing the overlaps between the reads and the genome annotation. The reads were assigned to a gene if they covered it by at least 10 bp (on the same strand). If the read contained more than one gene, the most upstream gene was counted, as this will be translated. The R scripts that were used in the downstream analysis are available at the following GitHub link: https://github.com/Balays/Rlyeh. Reads mapped on the KSHV genome have been deposited in the European Nucleotide Archive under the accession number PRJEB64045.

Cleavage under targets and release using nuclease

SLK cells were treated with 250 µM $CoCl_2$ for 16 h, followed by KSHV infection for 72 h. The CUT&RUN assay was carried out based on the manufacturer's instructions (Cell Signaling Technology). Primers used in the qPCR analysis of cleavage under targets and release using nuclease (CUT&RUN) samples are listed in Table 1. Then, 200,000 cells and 1 µg of HIF-1α antibody were used for each reaction.

siRNA knockdown

HIF-1α siRNA was purchased from Santa Cruz Biotechnology (sc-35561). Lipofectamine RNAiMAX (Invitrogen) was used for siRNA transfection, which was performed according to the manufacturer's instructions.

Lentiviruses production and transduction

The N-terminal 3xFLAG-tagged HIF-1α wild type (WT) and its mutants were expressed from the pCDHCMV-MCS-EF1puro lentiviral vector. Lentiviral vectors with 3xFLAG HIF-1α and its mutants were generated by in-fusion cloning (Takara). The lentivirus production and lentivirus transduction were performed as described previously (26). Two days after lentivirus transduction, the cells were split, and the same number of lentivirus-transduced cells was infected with KSHV.

Total RNA and DNA isolation and their qPCR analysis

RNA and DNA extractions and their qPCR analysis were performed as described in our previous publication (26). In the RT-qPCR analysis of gene expression, 18S RNA

TABLE 1 List of primers used in this study

Gene	Forward (5′-3′)	Reverse (5′-3′)	Application
RTAgb	ACACTGTACCAGCTGCACCA	GAAGTTAACGCAGGCACAGAC	RT-qPCR
ORF36	ATTGCCAACGACCTGATGCA	ACTCCAGTCCAGCTGCAGCA	RT-qPCR
ORF56	CACAGATTCCCGTCAATACAAA	GTATCTTCAGTAGGCGGCAGAG	RT-qPCR
ORF25gb	ACAGTTTATGGCACGCATAGTG	GGTTCTCTGAATCTCGTCGTGT	RT-qPCR
ORF64	CTTCCTCGAGGGCATCATATAC	TATACGGTGATGGACTTGATGG	RT-qPCR
ORF48	CCACATCTTCATAGAGCACAT	ATTGCATCACCAGGGTATCCA	RT-qPCR
RTA (HRE1)	ATGTGCGCGTATCCGGGCAAGCA	ACACGCCCTGGCGATTTTGGGTA	CUT&RUN-qPCR
RTA (HRE2)	TCAGGAGAGTTAGGGACGTGCTG	ACAGCTGTCGTTCAGATGTACCA	CUT&RUN-qPCR
RTA (HRE3)	AAGGTATAGGGTCTTCTCAACGT	AGTTAGATACCCTGTCCGTCG	CUT&RUN-qPCR
ORF34	CCTGGTACTCGACCAGTTGATCG	ACATACTTGCAGATGCGGTGTGT	CUT&RUN-qPCR
LANApr	GTTTATAAGTCAGCCGGACCAA	GATATAACTCCGCCCTCCACTA	ChIP-qPCR
RTApr (−0.6 kb)	AAGACACTGACCCACCAAGG	GGTGCCACCAATGTATGACC	ChIP-qPCR
K2pr	CATACGCAGCCAAGCTATCA	GCTAGCACAGCAAATTGAGA	ChIP-qPCR
ORF25pr	AGTTGTCGGTGTCTATCTGT	TGCAGAGCGATACGCAGACT	ChIP-qPCR
ORF11	GGCACCCATACAGCTTCTACGA	CGTTTACTACTGCACACTGCA	qPCR
HS1	TTCCTATTTGCCAAGGCAGT	CTCTTCAGCCATCCCAAGAC	qPCR
18S	TTCGAACGTCTGCCCTATCAA	GATGTGGTAGCCGTTTCTCAGG	RT-qPCR
VEGF	TGCAGATTATGCGGATCAAACC	TGCATTCACATTTGTTGTGCTGTAG	RT-qPCR

expression was used for normalization. The viral DNA level was measured by qPCR using KSHV ORF11-specific primers. Viral DNA was normalized to the cellular DNA level, which was measured using HS1-specific primers. The primers for KSHV and the host genes are listed in 5′ to 3′ orientation in Table 1. The RT-qPCR and qPCR results were calculated from the average of three independent experiments. To test statistical significance, we used a two-tailed Student's *t*-test, where $P < 0.05$ was considered significant.

Chromatin immunoprecipitation assay

The chromatin immunoprecipitation (ChIP) assay was performed as we have previously published (26). Then, 2 µg of chromatin and 0.5 µg of antibodies were used for each ChIP sample. The ChIP graphs show the average of three independent ChIP experiments. H3 occupancy was calculated as the percentage of the immunoprecipitated DNA compared to the input DNA. The level of histone marks was normalized by the histone H3 level at the indicated genomic sites. The ChIP-qPCR primer sequences are shown in Table 1.

Formaldehyde-assisted isolation of regulatory elements assay

The formaldehyde-assisted isolation of regulatory elements (FAIRE) analysis was performed as previously described (29). DNA was extracted from both formaldehyde-crosslinked and de-crosslinked chromatins and analyzed by qPCR using KSHV gene-specific primers. DNA purified from formaldehyde-crosslinked chromatin represents chromatin-free DNA, while DNA extracted from de-crosslinked chromatin represents total DNA. The level of chromatinization of viral genomic regions is shown by the ratio of chromatin-free DNA to total DNA.

Luciferase reporter assay

The luciferase reporter plasmid for hypoxia signaling was purchased from Addgene (#26731; HRE-luciferase). The RTA promoter luciferase plasmid was generated by cloning a 3-kb DNA sequence upstream of the ATG of the ORF50 gene into the pGL4.15 luciferase reporter vector. HEK293T cells in 24-well plates were transfected with a luciferase reporter plasmid together with plasmids expressing HIF-1α or its mutants. The transfection was carried out with polyethylenimine. At 48 h post-transfection, the cells were lysed in 200 µL of 0.5% Triton-X100 in PBS. Lysates were mixed with ONE-Glo luciferase substrate (Promega), and the luciferase activity was measured by the Promega GloMax-Multi detection system. All luciferase assays were carried out three times in triplicate. To test statistical significance, we used a two-tailed Student's *t*-test, where $P < 0.05$ was considered significant.

RESULTS

Hypoxia promotes the KSHV lytic cycle during primary infection

To test the effect of hypoxia on *de novo* KSHV infection, we first pre-treated SLK cells with the hypoxia mimetic agent $CoCl_2$ for 16 h and then infected the cells with KSHV in the presence of $CoCl_2$ for 24 and 72 h. $CoCl_2$ is known to be able to induce a hypoxia-like state by blocking the degradation of HIF-1α protein, resulting in its accumulation in cells and increased HIF-1α-mediated gene expression (30). For infection, we used the recombinant KSHV clone BAC16, which constitutively expresses GFP (31). Figure 1A shows that compared to KSHV-infected untreated cells, KSHV infection of $CoCl_2$-treated SLK cells resulted in increased cell rounding at 72 hpi, which was reminiscent of a cytopathic effect due to lytic infection. In line with this observation, when we infected $CoCl_2$-treated cells with the reporter virus rKSHV.219, which constitutively expresses GFP and an RTA-inducible RFP reporter gene for showing lytic phase (32), we observed increased RFP^+ cells indicating lytic viral infection (Fig. 1B). This observation was further supported by the immunofluorescence analysis showing the expression of the lytic viral protein ORF45 in nearly 15% of KSHV-infected $CoCl_2$-treated cells, while ORF45 was

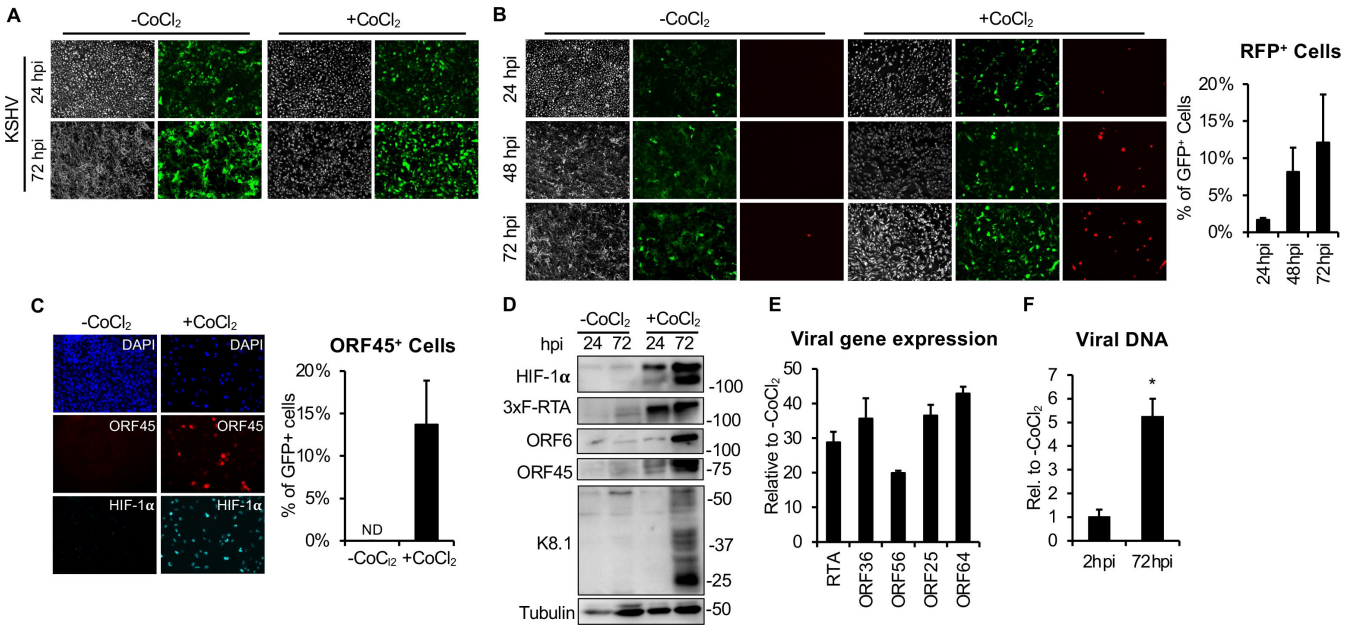

FIG 1 Induction of viral lytic gene expression by the hypoxia mimetic agent $CoCl_2$ during *de novo* KSHV infection. SLK cells were infected with KSHV in the absence or presence of $CoCl_2$. (A) Fluorescence microscope imaging of KSHV-infected cells at 24 and 72 hpi. GFP^+ cells show KSHV-BAC16-infected cells. (B) Fluorescence microscope imaging of SLK cells infected with rKSHV.219 at indicated time points. GFP shows KSHV infection of the cells, while RFP indicates the induction of lytic gene expression. RFP^+ cells were counted by ImageJ on five independent fields. (C) Immunofluorescence images showing the expression of the lytic viral proteins ORF45 (red) and HIF-1α (cy5) at 40 hpi. $ORF45^+$ cells were counted by ImageJ on three independent fields. ND, not detected. (D) Immunoblot analysis of HIF-1α and viral protein expression. (E) RT-qPCR analysis of viral gene expression at 72 hpi. The relative fold change represents the induction of viral gene expression in $CoCl_2$-treated cells relative to untreated cells. (F) Viral DNA levels at 2 and 72 hpi were measured by qPCR. A Student's *t*-test was performed between untreated and $CoCl_2$-treated samples (*, $P < 0.05$).

undetectable in the KSHV-infected untreated cells (Fig. 1C). Immunoblot analysis showed that the $CoCl_2$ treatment of cells during *de novo* KSHV infection increased HIF-1α protein level and the production of viral proteins (Fig. 1D), whereas RT-qPCR analysis showed increased transcription of viral lytic genes (Fig. 1E). We also found that while the viral DNA level was comparable between control and $CoCl_2$-treated SLK cells at 2 hpi, the amount of viral DNA was increased by more than fivefold in $CoCl_2$-treated infected cells at 72 hpi (Fig. 1F). These results demonstrated that the hypoxia mimetic agent $CoCl_2$ induces a viral lytic cycle during *de novo* KSHV infection.

Next, we assessed the effect of hypoxia on primary KSHV infection by pre-incubating SLK cells at a 1% O_2 level (hypoxia) for 16 h and then infecting them with KSHV under hypoxia (Fig. 2). Our results showed that hypoxia increased viral gene expression and viral protein production concomitantly with an increased HIF-1α protein level (Fig. 2A and B). KSHV infection under hypoxia also resulted in lytic viral DNA replication, which could be inhibited with the viral polymerase inhibitor PAA (Fig. 2C and D). Based on a supernatant transfer assay, we also detected a substantial amount of infectious viruses in the media of cells that were infected under hypoxia (Fig. 2E). Time-course KSHV infection of cells under hypoxia showed that viral lytic gene expression was increased as early as 8 hpi compared to viral infection under normoxia, which further supports the notion that hypoxia allows lytic *de novo* infection (Fig. 2F and G). Finally, we also tested the effect of hypoxia on KSHV primary infection in several biologically relevant endothelial cell types in which KSHV establishes latency after infection under normoxia (33, 34). We infected human umbilical vein cells (EA.hy926), immortalized lung microvascular endothelial cells (HULEC-5a), immortalized dermal microvascular endothelial cells (HMEC-1), and telomerase-immortalized human microvascular endothelial cells (TIME) with KSHV under normoxia and hypoxia. We found that hypoxia induced viral lytic gene expression in all tested endothelial cell lines following *de novo* KSHV infection (Fig. 2H).

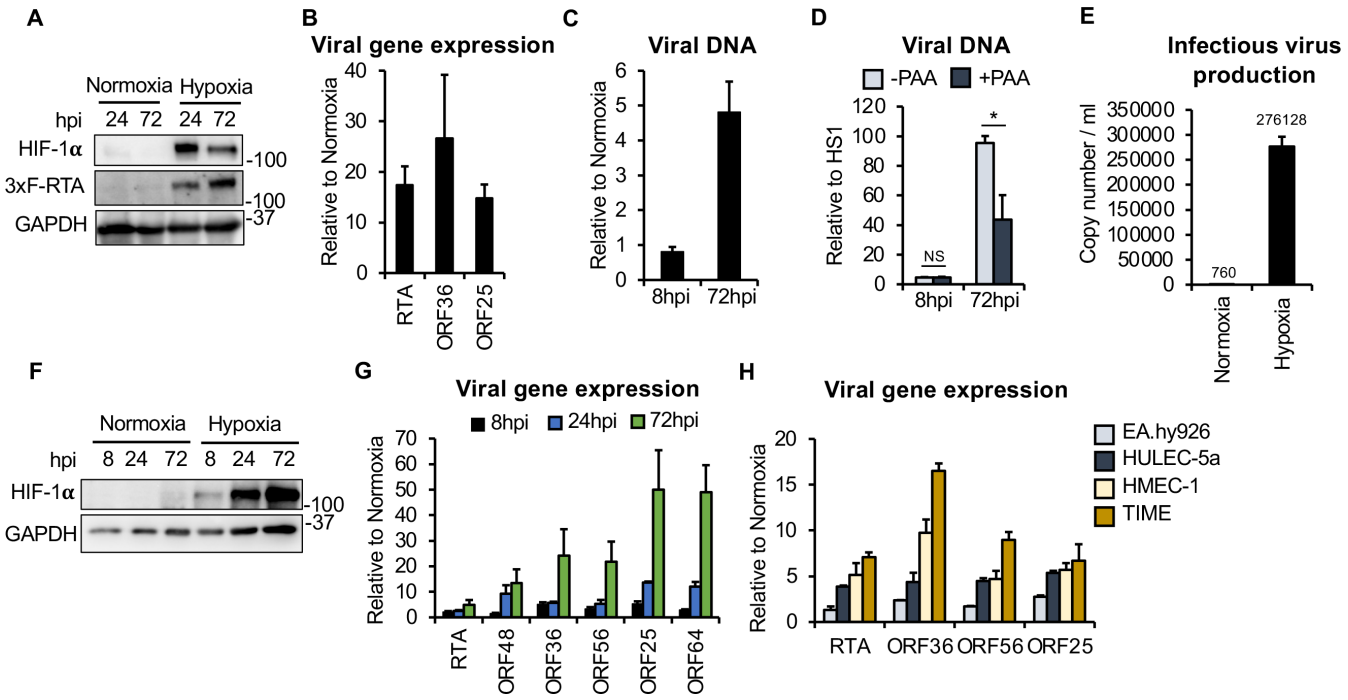

FIG 2 Lytic infection of cells by KSHV under hypoxia. Cells were infected with KSHV under normoxia and hypoxia. (A) Immunoblot analysis of HIF-1α and RTA expressed by KSHV BAC16-3xFLAG-RTA in SLK cells. (B) RT-qPCR analysis of viral gene expression. (C) Viral DNA levels at 8 and 72 hpi were measured by qPCR. (D) SLK cells were infected with KSHV in the presence or absence of 100 µM PAA for 8 and 72 hpi under hypoxia. The viral DNA level was measured by qPCR. (E) Supernatants from KSHV-infected SLK cells incubated under hypoxia or normoxia were used to infect fresh SLK cells for 24 h. The amount of infectious virus in the supernatant was calculated based on the level of viral DNA in cells after infection, which was measured by qPCR. (F) SLK cells were infected with KSHV for 8, 24, and 72 h, and HIF-1α expression was detected by immunoblotting. The relative fold change represents the induction of viral gene expression in hypoxia samples relative to cells cultured under normoxia at different time points of KSHV infection. (G) RT-qPCR analysis of viral gene expression in samples that are shown in panel E. (H) The indicated endothelial cells were infected with KSHV for 3 days. Viral gene expression was measured by RT-qPCR. The relative fold change represents the induction of viral gene expression in hypoxia samples relative to cells cultured under normoxia. A Student's *t*-test was performed between untreated and PAA-treated samples (*, $P < 0.05$). NS, not significant.

Altogether, our data indicate that hypoxia allows lytic *de novo* infection in cells, in which normally KSHV establishes latency following infection in a stress-free environment.

Genome-wide analysis of KSHV gene expression during primary infection under hypoxia

To determine if hypoxia globally induces viral gene expression during primary infection, we infected SLK cells with KSHV under normoxia and hypoxia and performed nanopore sequencing at 72 hpi (Fig. 3). Because this experiment was performed using a hypoxia incubator, instead of doing a spinning infection, which can achieve nearly 100% infectivity, we had to do the infection by incubating the cells with media containing KSHV, which is a much less efficient way of doing KSHV infection. Therefore, we obtained fewer viral transcripts for nanopore sequencing, which favors the detection of more abundant viral transcripts. Nevertheless, in agreement with previous studies, we confirmed that KSHV infection of SLK under normoxia results in latency during which the latent genes (K12, viral miRNAs, ORF71, ORF72, ORF73) remain expressed while the transcription of lytic genes becomes largely limited in the latently infected cell population (35, 36). While the K12 RNA transcript was readily detectable in the normoxia samples, the detection of the expression of other latent genes such as ORF73 was more challenging, which can be due to their low expression, which was described by previous studies as well (Fig. 3) (35–37). Interestingly, we observed that a subset of lytic genes was detectable at a relatively high level in infected cells during normoxia (e.g.,

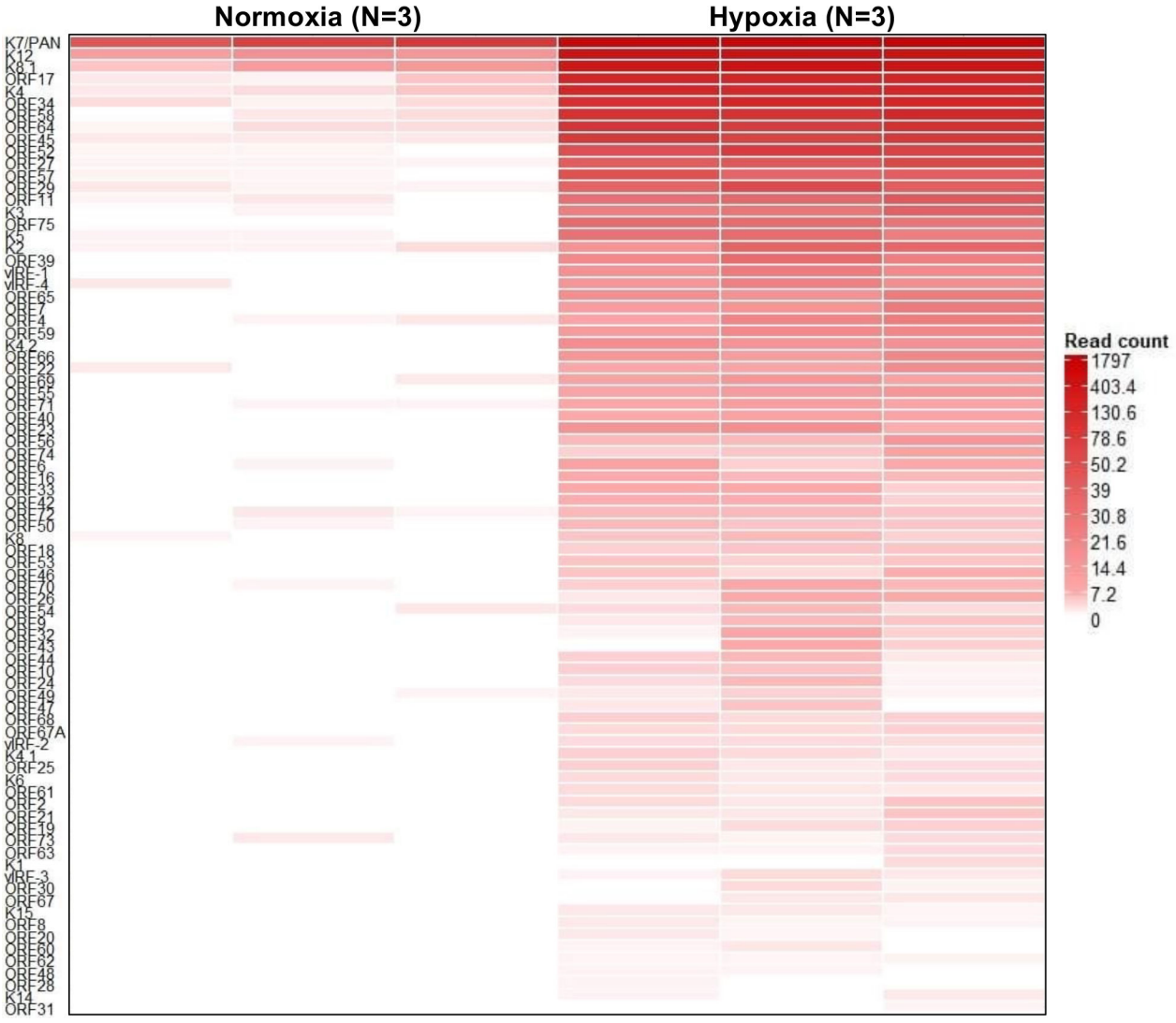

FIG 3 Genome-wide viral gene expression during *de novo* KSHV infection in hypoxia. SLK cells were infected with KSHV for 3 days under normoxia and hypoxia. PolyA(+) RNAs were purified from infected cells and subjected to nanopore sequencing.

K7/PAN, K8.1 ORF17, K4) (Fig. 3). This result corroborates previous viral transcriptome analyses, where the expression of these viral lytic genes was observed during primary KSHV infection in several human endothelial cell lines as well (35). In contrast to infection under normoxia, however, we found that hypoxia induces all viral genes during *de novo* KSHV infection (Fig. 3). This information further supports the notion that hypoxia allows the establishment of lytic KSHV infection.

Hypoxia-induced lytic *de novo* KSHV infection depends on the expression of RTA

RTA is known to be an essential viral transcription factor of KSHV that induces and drives the lytic gene expression cascade in the lytic phase (5, 38). However, since HIF-1α has been shown to be able to directly induce several lytic genes (24, 39, 40), it raises the question of how crucial RTA is for inducing lytic gene expression during *de novo* infection under hypoxia. To test whether the hypoxia-mediated induction of the lytic cycle requires RTA, we infected SLK cells with the same titer of WT and RTA-KO KSHV under normoxia and hypoxia (Fig. 4A) and analyzed viral and host gene expression at 72 hpi (Fig. 4B and D). Interestingly, we observed that the HIF-1α protein level was elevated

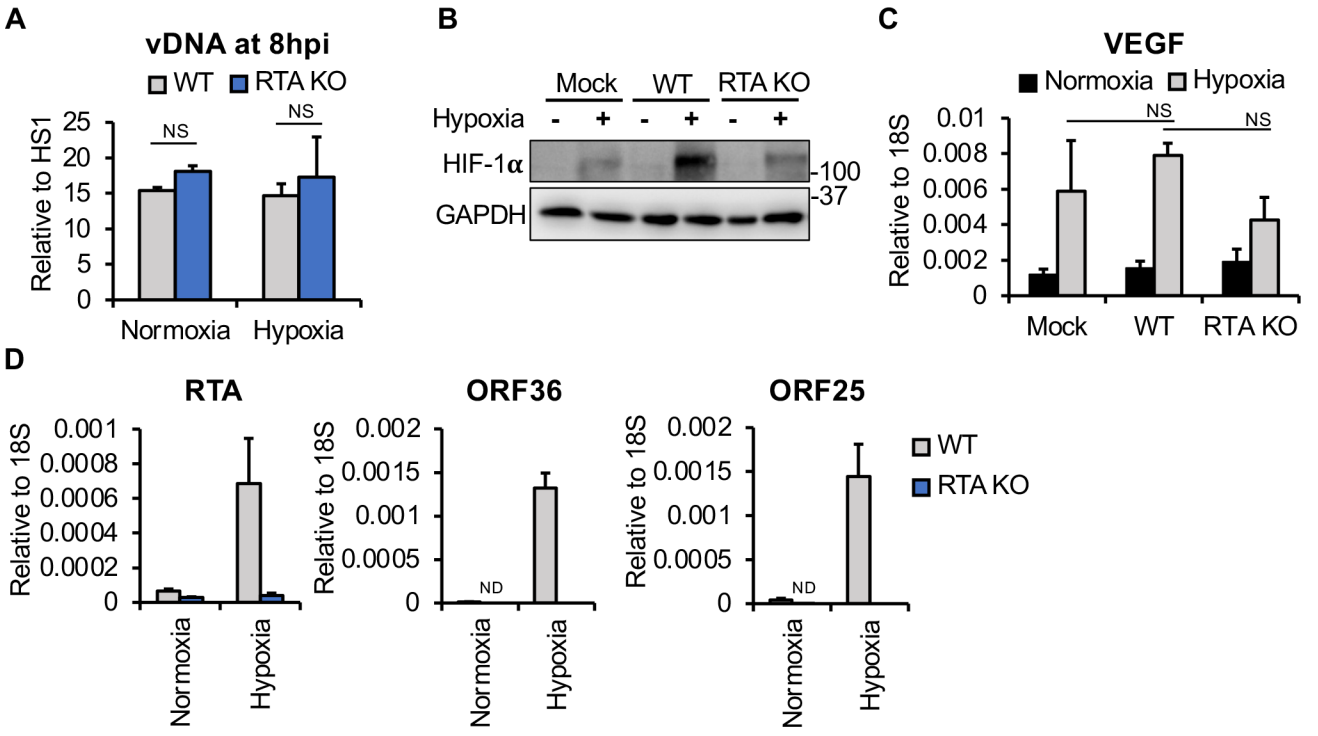

FIG 4 RTA is required for hypoxia-induced lytic *de novo* KSHV infection. SLK cells were infected with WT or RTA-KO KSHV for 3 days under normoxia and hypoxia. NS, not significant. (A) qPCR measurement of viral DNA level at 8 hpi. (B) Immunoblot detection of HIF-1α in uninfected (mock), WT, and RTA-KO KSHV-infected cells under normoxia and hypoxia. (C) RT-qPCR analysis of VEGF gene expression in mock, WT, and RTA-KO KSHV-infected cells under normoxia and hypoxia. (D) RT-qPCR analysis of the expression of lytic viral genes in WT and RTA-KO KSHV-infected cells at 72 hpi. ND, not detected. A Student's *t*-test was performed between WT and RTA-KO (A) as well as WT and mock or RTA-KO KSHV-infected cells (C).

in WT KSHV-infected cells but not in RTA-KO KSHV-infected cells compared to the mock sample under hypoxia (Fig. 4B). Our results also showed that while the expression of the hypoxia-induced HIF-1α target host gene VEGF was comparable between mock and KSHV-infected cells (Fig. 4C) (41), the hypoxia-induced lytic viral gene expression was abrogated in the RTA-KO KSHV-infected cells (Fig. 4D). This information indicates that RTA is required for robust lytic gene expression during infection in hypoxia. Our results also suggest that RTA and/or other lytic viral factors are involved in maintaining the high HIF-1α protein level during hypoxic lytic infection, which is in agreement with previous findings that several viral proteins can modulate HIF-1α protein abundance (12, 39, 42–44).

Hypoxia promotes euchromatin formation on the KSHV genome during *de novo* infection

It is known that the KSHV genome contains several hypoxia-responsive elements that can regulate hypoxia-induced viral gene expression. To measure the binding of HIF-1α to HREs in viral gene promoters during *de novo* infection in hypoxia, a CUT&RUN assay was performed in $CoCl_2$-treated SLK cells at 72 hpi. We detected an enrichment of HIF-1α on three known HREs at the RTA gene and on one known HRE in the promoter of the ORF34 gene upon $CoCl_2$ treatment, indicating that HIF-1α can play a role in the upregulation of lytic genes during hypoxic infection (Fig. 5A). Next, to determine the effect of hypoxia on KSHV chromatinization during *de novo* infection, FAIRE assays and ChIP experiments were performed with $CoCl_2$-treated SLK cells that were infected with KSHV for 72 h. We used RTA-KO KSHV to exclude the effect of $CoCl_2$-induced RTA on the chromatinization of KSHV DNA during *de novo* infection. We found that the $CoCl_2$-treatment resulted in less chromatinized DNA at the lytic RTA, K2, and ORF25 promoters, which drives

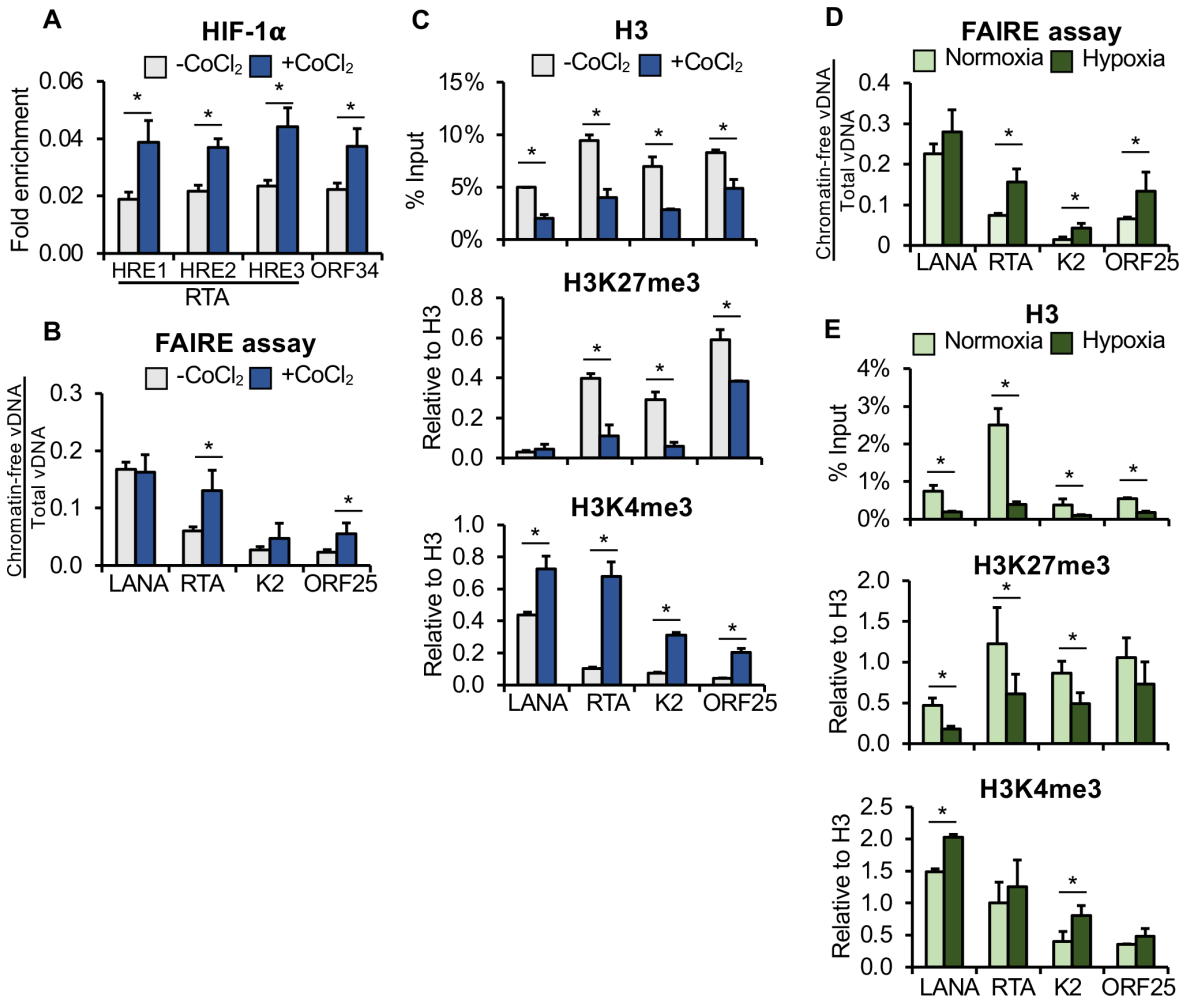

FIG 5 Analysis of the effect of hypoxia on the chromatinization of the KSHV genome during *de novo* infection. Hypoxia was induced by $CoCl_2$ treatment (A–C), or the cells were exposed to hypoxia (D–E). (A) CUT&RUN analysis to detect the binding of HIF-1α on HREs in the promoters of the RTA and ORF34 genes. (B) FAIRE assay to analyze the level of chromatin-free DNA at KSHV promoters. (C) ChIP analysis to measure H3 occupancy and the enrichment of H3K27me3 and H3K4me3 on viral promoters. (D) FAIRE assay to measure the level of chromatin-free DNA at the indicated viral promoters. (E) ChIP analysis of H3 occupancy and the enrichment of H3K27me3 and H3K4me3 on viral promoters. A Student's *t*-test was performed between untreated and $CoCl_2$-treated samples (A–C) as well as between normoxia and hypoxia samples (D–E) (*, $P < 0.05$).

the expression of an IE, E, and L viral gene, respectively (Fig. 5B). In agreement with this, the ChIP assay showed reduced histone H3 occupancy and reduced enrichment of the repressive histone mark H3K27me3 on the viral promoters, while the level of the activating histone mark H3K4me3 was increased (Fig. 5C). Importantly, the FAIRE and ChIP assays that were performed with cells infected with KSHV under hypoxia showed comparable results to those of the $CoCl_2$ experiments (Fig. 5D and E). Altogether, these experiments demonstrated that hypoxia promotes the formation of a transcriptional active chromatin on the KSHV genome during *de novo* infection, which can favor the expression of lytic genes.

HIF-1α is required for hypoxia-induced lytic gene expression during *de novo* infection

Since HIF-1α is the master transcription regulator of the hypoxia stress response, we tested the necessity of HIF-1α for the hypoxia-induced KSHV lytic cycle during primary infection. To this end, we performed HIF-1α siRNA knockdown in $CoCl_2$-treated or

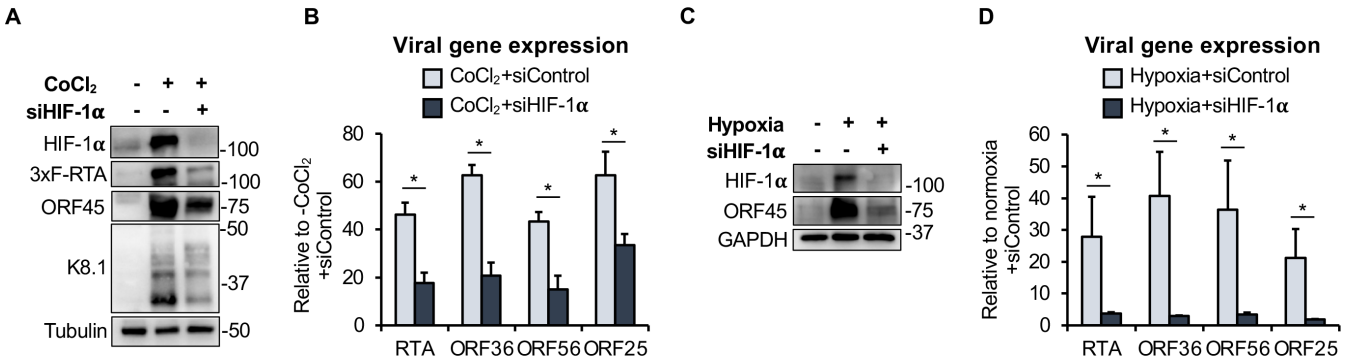

FIG 6 HIF-1α is essential for hypoxia-induced lytic primary KSHV infection. (A) SLK cells were transfected with 30 nM siControl or siHIF-1α for 16 h, followed by 250 µM $CoCl_2$ treatment for 16 h, and then infected with KSHV BAC16-3xFLAG-RTA for 3 days. Immunoblot detection of HIF-1α and viral proteins. (B) RT-qPCR analysis of viral gene expression in samples shown in panel A at 72 hpi. (C) SLK cells were transfected with 30 nM siControl of siHIF-1α for 16 h under hypoxia and then infected with KSHV for 3 days. Immunoblot detection of HIF-1α and the viral protein ORF45. (D) Viral gene expression in samples shown in panel C was measured by RT-qPCR. A Student's *t*-test was performed between the siControl and siHIF-1α samples (*, $P < 0.05$).

hypoxia-exposed *de novo* KSHV-infected cells, and viral gene expression and viral protein production were analyzed at 72 hpi (Fig. 6). Immunoblots showed robust viral protein production (RTA, ORF45, and K8.1) when HIF-1α was induced, while siHIF-1α treatment abrogated viral protein expression (Fig. 6A and C). In line with the immunoblot data, RT-qPCR analysis showed that hypoxia failed to induce viral gene expression in the absence of HIF-1α (Fig. 6B and D). These results demonstrate that HIF-1α is indispensable for hypoxia-induced viral lytic gene expression during *de novo* KSHV infection.

HIF-1α can support lytic primary infection by KSHV under normoxia

HIF-1α is a transcription factor consisting of 826 amino acids that possesses several functional domains that are crucial for its gene regulatory activity (Fig. 7A). Importantly, the hydroxylation of two proline residues (Pro402 and Pro564) located in its oxygen-dependent degradation domain is required for the interaction of HIF-1α with the VHL complex, which induces the degradation of HIF-1α under normoxia (45). Since HIF-1α is essential for hypoxia-induced lytic *de novo* KSHV infection, we wondered if HIF-1α expression alone can promote lytic viral gene expression during *de novo* infection under normoxia. To test this, we first analyzed the expression and transcriptional activity of overexpressed 3xFLAG-tagged HIF-1α under normoxia. We transfected 293T cells with 3xFLAG-HIF-1α (wild type) and 3xFLAG-HIF-1αSt (St for stabilized), which contain point mutations at Pro402 and Pro564, to prevent its degradation by VHL, resulting in its stabilization under normoxia (Fig. 7B). We evaluated the transactivation function of HIF-1α and HIF-1αSt with luciferase reporter assays using luciferase reporter plasmids that contained a minimal promoter coupled with HREs or contained the RTA promoter, which has several HREs (39). Interestingly, we found that HIF-1α WT and HIF-1αSt can induce the HRE and the RTA promoter luciferase reporter plasmids at a similar level (Fig. 7C), despite the fact that the HIF-1αSt protein level was higher than WT HIF-1α (Fig. 7B). Next, we infected SLK cells overexpressing GFP (negative control), 3xFLAG-HIF-1α, or 3xFLAG-HIF-1αSt with KSHV to test if HIF-1α supports lytic *de novo* KSHV infection. Immunoblotting in Fig. 7D and RT-qPCR analysis in Fig. 7E show that both 3xFLAG-HIF-1α and 3xFLAG-HIF-1αSt induced viral gene expression and viral protein production in *de novo* KSHV-infected cells at 24 and 72 hpi under normoxia. We note, however, that 3xFLAG-HIF-1αSt, whose expression was higher, induced higher lytic gene expression relative to 3xFLAG-HIF-1α. Collectively, these results support the notion that HIF-1α expression is sufficient to support lytic primary KSHV infection under normoxia.

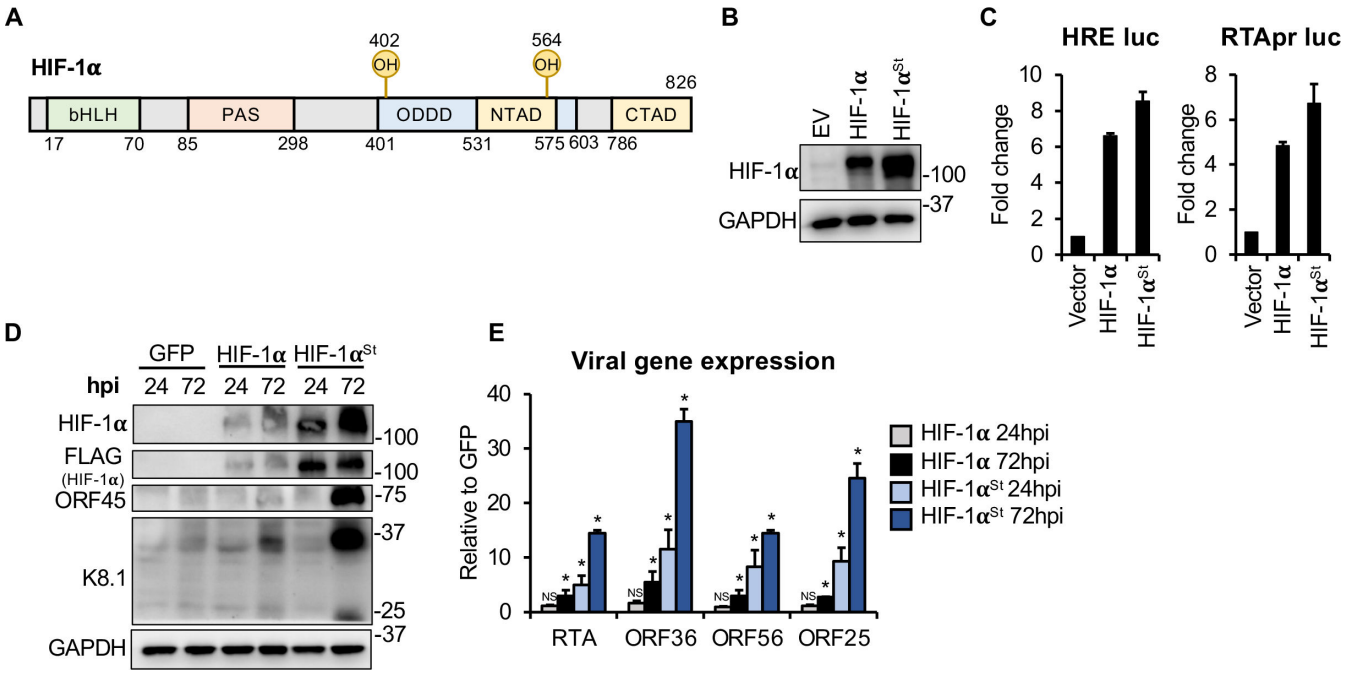

FIG 7 HIF-1α is sufficient to induce KSHV lytic gene expression during *de novo* infection under normoxia. (A) Schematic of HIF-1α domain structure. (B) FLAG immunoblot analysis of 3xFLAG-HIF-1α and 3xFLAG-HIF-1αSt expression in transfected HEK293T cells. (C) HEK293T cells were co-transfected with vector control, 3xFLAG-HIF-1α or 3xFLAG-HIF-1αSt, along with luciferase reporter plasmids containing a minimal promoter coupled with HRE or containing the RTA promoter. The fold change was calculated by comparing HIF-1α-induced luciferase activity to the basal activity of the luciferase reporter plasmids with vector control. (D) SLK cells were transduced with lenti-GFP (negative control), lenti-3xFLAG-HIF-1α, or lenti-3xFLAG-HIF-1αSt for 3 days, followed by KSHV infection for 24 and 72 h. The expression of HIF-1α and viral proteins was detected by immunoblotting. (E) RT-qPCR analysis of viral gene expression relative to KSHV-infected cells with lenti-GFP. A Student's *t*-test was performed between GFP and HIF-1α or GFP and HIF-1αSt samples at the indicated time points (*, $P < 0.05$). NS, not significant.

Evaluating the role of HIF-1α functional domains in HIF-1α-induced lytic KSHV infection

The N-terminus of HIF-1α contains a basic-helix-loop-helix (bHLH) domain and the PER-ARNT-SIM (PAS) domain, which have DNA binding functions and dimerization properties, respectively (20, 46). Also, HIF-1α has two transactivation domains [N-terminal" transactivation domain (NTAD) and C-terminal transactivation domain (CTAD)] at its C-terminus, which are responsible for its transcriptional activity (20, 47). To investigate what domains of HIF-1α are required for HIF-1α-induced *de novo* lytic KSHV infection, we constructed a series of HIF-1α truncation mutants. We deleted the DNA binding domain (ΔDB), the N- and C-terminal transactivation domains (ΔNTAD, ΔCTAD, and ΔTAD) of HIF-1α and made a dominant negative form of HIF-1α (DomNeg), which can dimerize with HIF-1β but lost its DNA binding activity, rendering it transcriptionally inactive (Fig. 8A). In each of these mutants, the Pro402 and Pro564 residues were mutated to prevent them from being degraded under normoxia.

SLK cells expressing GFP (negative control), the full-length HIF-1α, or its different mutants were infected with KSHV for 72 h. Immunoblot analysis showed that the expression levels of full-length HIF-1α and its mutants were comparable (Fig. 8B). RT-qPCR analysis of the viral gene expression revealed that the induction of lytic genes was greatly reduced when the cells expressed the DomNeg, ΔDB, ΔNTAD, or ΔTAD mutant of HIF-1α during *de novo* KSHV infection. Surprisingly, however, the CTAD deletion mutant could still increase lytic gene expression during *de novo* infection as efficiently as full-length HIF-1α (Fig. 8C). We also examined the transcriptional activity of the HIF-1α mutants by luciferase reporter assays using the HRE and RTA promoter reporter plasmids (Fig. 8D). We found that while ΔNTAD and ΔCTAD mutants partially lost their transcriptional activity, the ΔDB, ΔTAD, and DomNeg mutants of HIF-1α failed to

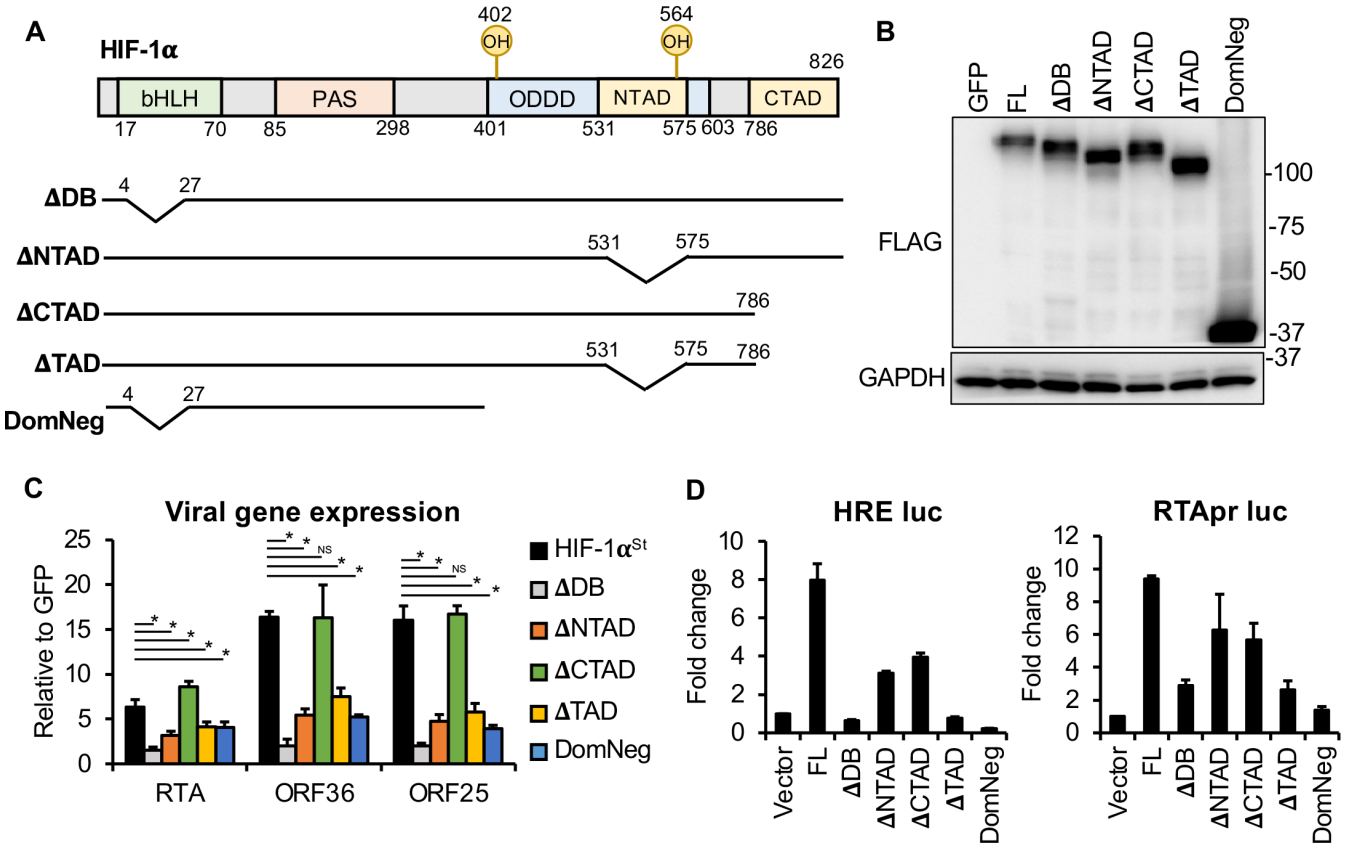

FIG 8 DNA-binding and NTAD domains are required for HIF-1α-induced lytic gene expression under normoxia. (A) Schematic of HIF-1α mutants. ΔDB, DNA-binding domain deletion. ΔNTAD, N-terminal transactivation domain deletion. ΔCTAD, C-terminal transactivation domain deletion. DomNeg, dominant negative form. (B) SLK cells were transduced with lenti-GFP (negative control), lenti-3xFLAG-HIF-1αSt (FL, full length), or the mutants for 3 days, followed by KSHV infection for 72 h. Immunoblot detection of HIF-1αSt and its mutants in the lentivirus-transduced, KSHV-infected cells. (C) RT-qPCR analysis of viral gene expression relative to lenti-GFP-transduced, KSHV-infected cells. A Student's *t*-test was performed between HIF-1αSt (FL) and HIF-1α mutants (*, $P < 0.05$). NS, not significant. (D) HEK293T cells were co-transfected with vector control, 3xFLAG-HIF-1αSt, or the HIF-1αSt mutants along with the indicated luciferase reporter plasmids. The fold change was calculated by comparing the luciferase activity of the samples to the basal activity of the luciferase reporter plasmids with vector control.

induce the HRE luciferase report plasmid (Fig. 8D). In contrast, only the DomNeg mutant lost its ability to induce the RTA promoter, while the other HIF-1α mutants could still induce the RTA promoter but at a much lower level relative to the full-length HIF-1α (Fig. 8D). Taken together, these results demonstrate that both the DNA-binding domain and the N-terminal transactivation domain of HIF-1α are crucial for facilitating lytic KSHV infection by inducing viral lytic gene expression during *de novo* infection.

DISCUSSION

KSHV infection *in vivo* occurs in a challenging environment in which cells are exposed to many different stress stimuli that can affect the outcome of primary KSHV infection, that is, whether the virus will establish latency or a lytic cycle after infection. However, the impact of the different natural stress conditions on primary KSHV infection has been understudied so far. In this study, we provided evidence for the natural stress stimulus hypoxia being able to induce lytic *de novo* infection in cells that would be latently infected by KSHV under normoxia (Fig. 1 through 4). We found that when KSHV infects cells under hypoxia, the formation of heterochromatin is reduced on the incoming viral DNA (Fig. 5), which can favor lytic gene expression and viral DNA replication. Also, our data show that HIF-1α is crucial for not only the hypoxia-induced lytic KSHV infection (Fig. 6), but HIF-1α alone is sufficient to allow robust lytic viral gene expression during

de novo infection (Fig. 7), which requires HIF-1α's DNA-binding and N-terminal transactivation domains (Fig. 8). Based on our results, we propose that cellular stress responses during *de novo* infection can determine how KSHV infects cells and whether the virus will establish latency or lytic infection. In this regard, a recent study demonstrated that HIF-1α is necessary for the robust lytic infection of mice with the murine gammaherpesvirus 68, which supports our notion that HIF-1α could also regulate the lytic KSHV infection of humans (48).

Previous studies have demonstrated that hypoxia can induce lytic reactivation of KSHV in latently infected cells and promote the growth of KSHV$^+$ PEL cells (11–13, 39, 42, 44, 49). The lytic reactivation-inducing ability of hypoxia was accounted for by HIF-1 binding to HREs that are found in viral promoters, which can induce the expression of RTA and other lytic genes, resulting in viral replication (23, 24). ChIP-seq analysis showed that HIF-1α is enriched at several loci on the KSHV genome in hypoxia-exposed KSHV-infected PBMC and KSHV$^+$ BC3 cells (42). In line with previous lytic reactivation studies, we showed by the CUT&RUN assay that HIF-1α binds to HREs in viral promoters, suggesting that HIF-1α could regulate lytic gene expression also during *de novo* infection in hypoxia (Fig. 5A). In addition, our ChIP analysis demonstrated that during hypoxic KSHV infection compared to infection under normoxia, the viral DNA has more open chromatin, and there is an enrichment of activating histone marks and a reduced level of the repressive histone mark H3K27me3 on the lytic promoters (Fig. 5). Such viral chromatin changes have been shown to favor lytic gene expression that can lead to viral DNA replication, which can also be observed during *de novo* infection in hypoxia (Fig. 1 through 3) (50–52). We also determined that HIF-1α is necessary but not sufficient to induce hypoxic lytic KSHV infection; in addition, RTA is required (Fig. 4). Nevertheless, we found that the higher the HIF-1α protein level is, the higher the expression of KSHV lytic genes is, supporting the importance of HIF-1α in the regulation of lytic KSHV infection (Fig. 7). Interestingly, we also noticed that the HIF-1α protein level was reduced in cells infected with the lytic cycle-deficient RTA-KO KSHV compared to cells infected with WT KSHV during hypoxia. This implies that RTA and/or some other lytic factors of KSHV are needed to maintain the high HIF-1α level during hypoxic lytic infection. In this regard, previous studies have demonstrated that several KSHV factors can modulate the expression of HIF-1α at the protein or mRNA levels or affect its transcriptional activity (11, 39, 43, 53, 54). What viral factors play a role in HIF-1α induction in hypoxic lytic *de novo* KSHV infection, however, remains unknown, but we are going to address it in future studies. Overall, based on our data, we propose that there is a positive feedback loop between the expression of KSHV lytic genes and HIF-1α, facilitating KSHV lytic infection under hypoxia.

Is any expression of HIF-1α sufficient to induce robust lytic *de novo* KSHV infection? This is probably not the case. Our fluorescence microscopy analysis showed that there is heterogeneity not only in viral gene expression but also in HIF-1α expression in different cells in response to $CoCl_2$ treatment during primary infection (Fig. 1B and C). There is only a subset of cells showing RFP$^+$ signal or ORF45 expression during $CoCl_2$-incubation, despite the fact that more than 99% of cells are infected (data not shown), while all cells show HIF-1α expression, although at different levels. This observation suggests a heterogenic primary KSHV infection under hypoxic conditions, which correlates with a single-cell analysis study showing heterogenous viral gene expression in KSHV-infected cells of oral epithelial organoids as well (37). Several previous studies have also demonstrated that not all latently infected KSHV$^+$ cells undergo the same level of viral reactivation when all cells are exposed to a potent lytic cycle inducer (55–57). In agreement with previous studies, our results support the notion that the transcriptome or proteomic profile of different infected cells may determine the output of lytic gene expression and virus production in an individual infected cell. As a matter of fact, we speculate that the variance in the hypoxia-induced activation of viral genes in different endothelial cell lines can also be due to variable HIF-1α protein abundance and/or

different levels of HIF-1α-associated co-activators across the different cell lines (Fig. 2H). However, this needs further investigation.

HIF-1α has multiple functional domains that are crucial for the activation of various cellular promoters. Besides the N-terminal bHLH DNA-binding domain, HIF-1α also contains two transactivation domains between amino acid residues 531 and 828, such as the CTAD and a more centrally located NTAD (Fig. 7A). We found that the DNA-binding domain and NTAD are essential for HIF-1α-mediated upregulation of viral lytic genes during *de novo* infection (Fig. 8). Interestingly, CTAD was dispensable for HIF-1α-induced lytic gene expression, despite the fact that both NTAD and CTAD are known to be involved in recruiting transcriptional co-activators to HIF-1α's target promoters (Fig. 8) (58, 59). However, it has been reported previously that the expression of a subset of HIF-1α's host target genes also requires only NTAD but not CTAD (60). Additionally, another group constructed a HIF-1α/HIF-2α chimeric protein by swapping their NTAD or CTAD and investigating their transcriptional activity on endogenous HIF-1′s host target genes. They found that while both NTAD and CTAD are necessary for optimal HIF transcriptional activity, NTAD confers HIF target gene specificity (61). We note that while both NTAD and CTAD seem to be necessary for the full transcriptional activity of HIF-1α in the HRE and RTA promoter luciferase reporter assays, only NTAD was required for the expression of lytic viral genes from the KSHV genome (Fig. 8). We speculate that the discrepancy may be accounted for by the KSHV genome being chromatinized in contrast to the reporter plasmids, and that the co-activators that interact with HIF-1α in the context of the viral chromatin require NTAD rather than CTAD. Further analyses will be needed to dissect the mechanism of NTAD-dependent HIF-1α-induced KSHV lytic infection.

It was demonstrated that a number of different stress factors, such as certain chemicals, reactive oxidative species (ROS), inflammatory cytokines, and viral and bacterial co-infections, can also induce lytic reactivation of KSHV in latently infected cells (62, 63). Some of the stress signals that are known inducers of the KSHV lytic cycle, such as ROS, can also increase HIF-1α expression, raising the possibility that cells exposed to these stress signals may be able to support lytic KSHV infection via HIF-1α under normoxia (64). In line with this notion, we showed that HIF-1α expression under normoxia can substantially increase lytic gene expression during *de novo* KSHV infection, indicative of the establishment of lytic infection. In addition to hypoxia, several non-canonical mechanisms have been reported whereby HIF-1α protein levels can be upregulated under normoxia. For example, insulin and epidermal growth factor can increase the protein level of HIF-1α by activating the phosphatidylinositol 3-kinase and mitogen-activated protein kinase signaling pathways (65). Iron deprivation also leads to the stabilization of HIF-1α, since Fe^{2+} is an essential cofactor for PHD-mediated HIF-1α degradation (66). Whether any of these non-canonical pathways that can induce HIF-1α could also support HIF-1α-mediated lytic KSHV infection remains to be tested in future studies.

Interestingly, a recent study revealed that KSHV infection-associated host gene expression changes in SLK and endothelial cells show similarity to hypoxia-induced gene expression profiles in endothelial cells and host gene expression in AIDS-KS (67). In addition, HIF-1α was shown to play a role in regulating the cell metabolism of KS, the growth of PEL cells, and hypoxia-induced lytic reactivation (12, 13, 42, 67). Our study explored the impact of hypoxia and the expression of HIF-1α on *de novo* KSHV infection, and we found that they allow the establishment of lytic infection. Taken together, these studies support the notion that HIF-1α is critical for the regulation of the different stages of KSHV infection and viral pathogenesis, which makes HIF-1α and the hypoxia-related signaling pathways potential therapeutic targets for inhibiting KSHV infection and KSHV-associated diseases.

ACKNOWLEDGMENTS

This work was partly supported by an American Cancer Society Research Scholar Grant (RSG-18-221-01-MPC for Z.T. and B.P.) and the National Institutes of Health (R01AI132554 and R01DE028331 for Z.T. and B.P.).

This study was also supported by the National Research Development and Innovation Office (NRDIO) (grant numbers K 128247 and K 142674 for Z.B.). We thank Gary S. Hayward (Johns Hopkins University) for providing the ORF6 antibody. We would also like to thank members of the Papp and the Toth laboratories for the valuable discussions during the project.

AUTHOR AFFILIATIONS

[1]Department of Oral Biology, College of Dentistry, University of Florida, Gainesville, Florida, USA
[2]Department of Medical Biology, Albert Szent-Györgyi Medical School, University of Szeged, Szeged, Hungary
[3]UF Genetics Institute, Gainesville, Florida, USA
[4]UF Health Cancer Center, Gainesville, Florida, USA
[5]UF Center for Orphaned Autoimmune Disorders, Gainesville, Florida, USA
[6]UF Informatics Institute, Gainesville, Florida, USA
[7]Department of Molecular Genetics and Microbiology, College of Medicine, University of Florida, Gainesville, Florida, USA

AUTHOR ORCIDs

Zsolt Boldogkői http://orcid.org/0000-0003-1184-7293
Bernadett Papp http://orcid.org/0000-0001-5352-3946
Steeve Boulant http://orcid.org/0000-0001-8614-4993
Zsolt Toth http://orcid.org/0000-0001-6628-3945

FUNDING

Funder	Grant(s)	Author(s)
American Cancer Society (ACS)	RSG-18-221-01-MPC	Bernadett Papp Zsolt Toth
HHS | National Institutes of Health (NIH)	R01AI132554, R01DE028331	Zsolt Toth Bernadett Papp
National Research Development and Innovation Office	K128247, K142674	Zsolt Boldogkői

AUTHOR CONTRIBUTIONS

See-Chi Lee, Data curation, Formal analysis, Investigation, Writing – original draft, Writing – review and editing | Nenavath Gopal Naik, Formal analysis, Investigation, Writing – review and editing | Dóra Tombácz, Methodology, Resources | Gábor Gulyás, Methodology, Software | Balázs Kakuk, Methodology, Software | Zsolt Boldogkői, Data curation, Funding acquisition, Methodology, Project administration, Resources, Supervision, Writing – review and editing | Kevin Hall, Methodology | Bernadett Papp, Funding acquisition, Methodology, Visualization, Writing – review and editing | Steeve Boulant, Methodology, Resources | Zsolt Toth, Conceptualization, Data curation, Funding acquisition, Project administration, Supervision, Writing – review and editing

REFERENCES

1. Polizzotto MN, Uldrick TS, Hu D, Yarchoan R. 2012. Clinical manifestations of Kaposi sarcoma herpesvirus lytic activation: multicentric castleman disease (KSHV-MCD) and the KSHV inflammatory cytokine syndrome. Front Microbiol 3:73. https://doi.org/10.3389/fmicb.2012.00073

2. Chang Y, Cesarman E, Pessin MS, Lee F, Culpepper J, Knowles DM, Moore PS. 1994. Identification of herpesvirus-like DNA sequences in AIDS-associated Kaposi's sarcoma. Science 266:1865–1869. https://doi.org/10.1126/science.7997879
3. Oksenhendler E, Boutboul D, Galicier L. 2019. Kaposi sarcoma-associated herpesvirus/human herpesvirus 8-associated lymphoproliferative disorders. Blood 133:1186–1190. https://doi.org/10.1182/blood-2018-11-852442
4. Lukac DM, Kirshner JR, Ganem D. 1999. Transcriptional activation by the product of open reading frame 50 of Kaposi's sarcoma-associated herpesvirus is required for lytic viral reactivation in B cells. J Virol 73:9348–9361. https://doi.org/10.1128/JVI.73.11.9348-9361.1999
5. Sun R, Lin SF, Gradoville L, Yuan Y, Zhu F, Miller G. 1998. A viral gene that activates lytic cycle expression of Kaposi's sarcoma-associated herpesvirus. Proc Natl Acad Sci U S A 95:10866–10871. https://doi.org/10.1073/pnas.95.18.10866
6. Aneja KK, Yuan Y. 2017. Reactivation and lytic replication of Kaposi's sarcoma-associated herpesvirus: an update. Front Microbiol 8:613. https://doi.org/10.3389/fmicb.2017.00613
7. Giffin L, Damania B. 2014. KSHV: pathways to tumorigenesis and persistent infection. Adv Virus Res 88:111–159. https://doi.org/10.1016/B978-0-12-800098-4.00002-7
8. Bechtel JT, Liang Y, Hvidding J, Ganem D. 2003. Host range of Kaposi's sarcoma-associated herpesvirus in cultured cells. J Virol 77:6474–6481. https://doi.org/10.1128/jvi.77.11.6474-6481.2003
9. Carreau A, El Hafny-Rahbi B, Matejuk A, Grillon C, Kieda C. 2011. Why is the partial oxygen pressure of human tissues a crucial parameter? Small molecules and hypoxia. J Cell Mol Med 15:1239–1253. https://doi.org/10.1111/j.1582-4934.2011.01258.x
10. Zenewicz LA. 2017. Oxygen levels and immunological studies. Front Immunol 8:324. https://doi.org/10.3389/fimmu.2017.00324
11. Singh RK, Lamplugh ZL, Lang F, Yuan Y, Lieberman P, You J, Robertson ES, Chandran B. 2019. KSHV-encoded LANA protects the cellular replication machinery from hypoxia induced degradation. PLoS Pathog 15:e1008025. https://doi.org/10.1371/journal.ppat.1008025
12. Shrestha P, Davis DA, Veeranna RP, Carey RF, Viollet C, Yarchoan R. 2017. Hypoxia-inducible factor-1 alpha as a therapeutic target for primary effusion lymphoma. PLoS Pathog 13:e1006628. https://doi.org/10.1371/journal.ppat.1006628
13. Davis DA, Rinderknecht AS, Zoeteweij JP, Aoki Y, Read-Connole EL, Tosato G, Blauvelt A, Yarchoan R. 2001. Hypoxia induces lytic replication of Kaposi sarcoma-associated herpesvirus. Blood 97:3244–3250. https://doi.org/10.1182/blood.V97.10.3244
14. Chi J-T, Wang Z, Nuyten DSA, Rodriguez EH, Schaner ME, Salim A, Wang Y, Kristensen GB, Helland A, Børresen-Dale A-L, Giaccia A, Longaker MT, Hastie T, Yang GP, van de Vijver MJ, Brown PO. 2006. Gene expression programs in response to hypoxia: cell type specificity and prognostic significance in human cancers. PLoS Med 3:e47. https://doi.org/10.1371/journal.pmed.0030047
15. Wang GL, Semenza GL. 1993. General involvement of hypoxia-inducible factor 1 in transcriptional response to hypoxia. Proc Natl Acad Sci U S A 90:4304–4308. https://doi.org/10.1073/pnas.90.9.4304
16. Wang GL, Jiang BH, Rue EA, Semenza GL. 1995. Hypoxia-inducible factor 1 is a basic-helix-loop-helix-PAS heterodimer regulated by cellular O2 tension. Proc Natl Acad Sci U S A 92:5510–5514. https://doi.org/10.1073/pnas.92.12.5510
17. Huang LE, Gu J, Schau M, Bunn HF. 1998. Regulation of hypoxia-inducible factor 1alpha is mediated by an O2-dependent degradation domain via the ubiquitin-proteasome pathway. Proc Natl Acad Sci U S A 95:7987–7992. https://doi.org/10.1073/pnas.95.14.7987
18. Ivan M, Kondo K, Yang H, Kim W, Valiando J, Ohh M, Salic A, Asara JM, Lane WS, Kaelin WG. 2001. HIFalpha targeted for VHL-mediated destruction by proline hydroxylation: implications for O2 sensing. Science 292:464–468. https://doi.org/10.1126/science.1059817
19. Maxwell PH, Wiesener MS, Chang GW, Clifford SC, Vaux EC, Cockman ME, Wykoff CC, Pugh CW, Maher ER, Ratcliffe PJ. 1999. The tumour suppressor protein VHL targets hypoxia-inducible factors for oxygen-dependent proteolysis. Nature 399:271–275. https://doi.org/10.1038/20459
20. Jiang BH, Rue E, Wang GL, Roe R, Semenza GL. 1996. Dimerization, DNA binding, and transactivation properties of hypoxia-inducible factor 1. J Biol Chem 271:17771–17778. https://doi.org/10.1074/jbc.271.30.17771
21. Huang R, Huestis M, Gan ES, Ooi EE, Ohh M. 2021. Hypoxia and viral infectious diseases. JCI Insight 6. https://doi.org/10.1172/jci.insight.147190
22. Méndez-Solís O, Bendjennat M, Naipauer J, Theodoridis PR, Ho JJD, Verdun RE, Hare JM, Cesarman E, Lee S, Mesri EA. 2021. Kaposi's sarcoma herpesvirus activates the hypoxia response to usurp HIF2α-dependent translation initiation for replication and oncogenesis. Cell Rep 37:110144. https://doi.org/10.1016/j.celrep.2021.110144
23. Haque M, Wang V, Davis DA, Zheng ZM, Yarchoan R. 2006. Genetic organization and hypoxic activation of the Kaposi's sarcoma-associated herpesvirus ORF34-37 gene cluster. J Virol 80:7037–7051. https://doi.org/10.1128/JVI.00553-06
24. Haque M, Davis DA, Wang V, Widmer I, Yarchoan R. 2003. Kaposi's sarcoma-associated herpesvirus (human herpesvirus 8) contains hypoxia response elements: relevance to lytic induction by hypoxia. J Virol 77:6761–6768. https://doi.org/10.1128/jvi.77.12.6761-6768.2003
25. Toth Z, Brulois KF, Wong LY, Lee HR, Chung B, Jung JU. 2012. Negative elongation factor-mediated suppression of RNA polymerase II elongation of Kaposi's sarcoma-associated herpesvirus lytic gene expression. J Virol 86:9696–9707. https://doi.org/10.1128/JVI.01012-12
26. Toth Z, Smindak RJ, Papp B. 2017. Inhibition of the lytic cycle of Kaposi's sarcoma-associated herpesvirus by cohesin factors following *de novo* infection. Virology 512:25–33. https://doi.org/10.1016/j.virol.2017.09.001
27. Toth Z, Papp B, Brulois K, Choi YJ, Gao S-J, Jung JU, Dittmer DP. 2016. LANA-mediated recruitment of host polycomb repressive complexes onto the KSHV genome during *de novo* infection. PLoS Pathog 12:e1005878. https://doi.org/10.1371/journal.ppat.1005878
28. Tombácz D, Kakuk B, Torma G, Csabai Z, Gulyás G, Tamás V, Zádori Z, Jefferson VA, Meyer F, Boldogkői Z. 2022. In-depth temporal transcriptome profiling of an alphaherpesvirus using nanopore sequencing. Viruses 14:1289. https://doi.org/10.3390/v14061289
29. Lee S-C, Toth Z, Feng P. 2022. PRC1-independent binding and activity of RYBP on the KSHV genome during *de novo* infection. PLoS Pathog 18:e1010801. https://doi.org/10.1371/journal.ppat.1010801
30. Muñoz-Sánchez J, Chánez-Cárdenas ME. 2019. The use of cobalt chloride as a chemical hypoxia model. J Appl Toxicol 39:556–570. https://doi.org/10.1002/jat.3749
31. Brulois KF, Chang H, Lee AS-Y, Ensser A, Wong L-Y, Toth Z, Lee SH, Lee H-R, Myoung J, Ganem D, Oh T-K, Kim JF, Gao S-J, Jung JU. 2012. Construction and manipulation of a new Kaposi's sarcoma-associated herpesvirus bacterial artificial chromosome clone. J Virol 86:9708–9720. https://doi.org/10.1128/JVI.01019-12
32. Vieira J, O'Hearn PM. 2004. Use of the red fluorescent protein as a marker of Kaposi's sarcoma-associated herpesvirus lytic gene expression. Virology 325:225–240. https://doi.org/10.1016/j.virol.2004.03.049
33. An FQ, Folarin HM, Compitello N, Roth J, Gerson SL, McCrae KR, Fakhari FD, Dittmer DP, Renne R. 2006. Long-term-infected telomerase-immortalized endothelial cells: a model for Kaposi's sarcoma-associated herpesvirus latency *in vitro* and *in vivo*. J Virol 80:4833–4846. https://doi.org/10.1128/JVI.80.10.4833-4846.2006
34. Renne R, Blackbourn D, Whitby D, Levy J, Ganem D. 1998. Limited transmission of Kaposi's sarcoma-associated herpesvirus in cultured cells. J Virol 72:5182–5188. https://doi.org/10.1128/JVI.72.6.5182-5188.1998
35. Bruce AG, Barcy S, DiMaio T, Gan E, Garrigues HJ, Lagunoff M, Rose TM. 2017. Quantitative analysis of the KSHV transcriptome following primary infection of blood and lymphatic endothelial cells. Pathogens 6:11. https://doi.org/10.3390/pathogens6010011
36. Landis JT, Tuck R, Pan Y, Mosso CN, Eason AB, Moorad R, Marron JS, Dittmer DP. 2022. Evidence for multiple subpopulations of herpesvirus-latently infected cells. mBio 13:e0347321. https://doi.org/10.1128/mbio.03473-21
37. Jung KL, Choi UY, Park A, Foo S-S, Kim S, Lee S-A, Jung JU. 2022. Single-cell analysis of Kaposi's sarcoma-associated herpesvirus infection in three-dimensional air-liquid interface culture model. PLoS Pathog 18:e1010775. https://doi.org/10.1371/journal.ppat.1010775
38. Lukac DM, Renne R, Kirshner JR, Ganem D. 1998. Reactivation of Kaposi's sarcoma-associated herpesvirus infection from latency by expression of

the ORF 50 transactivator, a homolog of the EBV R protein. Virology 252:304–312. https://doi.org/10.1006/viro.1998.9486
39. Cai Q, Lan K, Verma SC, Si H, Lin D, Robertson ES. 2006. Kaposi's sarcoma-associated herpesvirus latent protein LANA interacts with HIF-1 alpha to upregulate RTA expression during hypoxia: latency control under low oxygen conditions. J Virol 80:7965–7975. https://doi.org/10.1128/JVI.00689-06
40. Veeranna RP, Haque M, Davis DA, Yang M, Yarchoan R. 2012. Kaposi's sarcoma-associated herpesvirus latency-associated nuclear antigen induction by hypoxia and hypoxia-inducible factors. J Virol 86:1097–1108. https://doi.org/10.1128/JVI.05167-11
41. Liu Y, Cox SR, Morita T, Kourembanas S. 1995. Hypoxia regulates vascular endothelial growth factor gene expression in endothelial cells. Identification of a 5' enhancer. Circ Res 77:638–643. https://doi.org/10.1161/01.res.77.3.638
42. Kumar Singh R, Pei Y, Bose D, Lamplugh ZL, Sun K, Yuan Y, Lieberman P, You J, Robertson ES. 2021. KSHV-encoded vCyclin can modulate HIF1α levels to promote DNA replication in hypoxia. Elife 10:e57436. https://doi.org/10.7554/eLife.57436
43. Shin YC, Joo CH, Gack MU, Lee HR, Jung JU. 2008. Kaposi's sarcoma-associated herpesvirus viral IFN regulatory factor 3 stabilizes hypoxia-inducible factor-1 alpha to induce vascular endothelial growth factor expression. Cancer Res 68:1751–1759. https://doi.org/10.1158/0008-5472.CAN-07-2766
44. Cai Q, Murakami M, Si H, Robertson ES. 2007. A potential alpha-helix motif in the amino terminus of LANA encoded by Kaposi's sarcoma-associated herpesvirus is critical for nuclear accumulation of HIF-1alpha in normoxia. J Virol 81:10413–10423. https://doi.org/10.1128/JVI.00611-07
45. Kamura T, Sato S, Iwai K, Czyzyk-Krzeska M, Conaway RC, Conaway JW. 2000. Activation of HIF1alpha ubiquitination by a reconstituted von hippel-lindau (VHL) tumor suppressor complex. Proc Natl Acad Sci U S A 97:10430–10435. https://doi.org/10.1073/pnas.190332597
46. Wang GL, Semenza GL. 1995. Purification and characterization of hypoxia-inducible factor 1. J Biol Chem 270:1230–1237. https://doi.org/10.1074/jbc.270.3.1230
47. Li H, Ko HP, Whitlock JP. 1996. Induction of phosphoglycerate kinase 1 gene expression by hypoxia. Roles of Arnt and HIF1alpha. J Biol Chem 271:21262–21267. https://doi.org/10.1074/jbc.271.35.21262
48. López-Rodríguez DM, Kirillov V, Krug LT, Mesri EA, Andreansky S. 2019. A role of hypoxia-inducible factor 1 alpha in murine gammaherpesvirus 68 (MHV68) lytic replication and reactivation from latency. PLoS Pathog 15:e1008192. https://doi.org/10.1371/journal.ppat.1008192
49. Davis DA, Shrestha P, Yarchoan R. 2023. Hypoxia and hypoxia-inducible factors in Kaposi sarcoma-associated herpesvirus infection and disease pathogenesis. J Med Virol 95:e29071. https://doi.org/10.1002/jmv.29071
50. Toth Z, Maglinte DT, Lee SH, Lee H-R, Wong L-Y, Brulois KF, Lee S, Buckley JD, Laird PW, Marquez VE, Jung JU. 2010. Epigenetic analysis of KSHV latent and lytic genomes. PLoS Pathog 6:e1001013. https://doi.org/10.1371/journal.ppat.1001013
51. Uppal T, Jha HC, Verma SC, Robertson ES. 2015. Chromatinization of the KSHV genome during the KSHV life cycle. Cancers (Basel) 7:112–142. https://doi.org/10.3390/cancers7010112
52. Fröhlich J, Grundhoff A. 2020. Epigenetic control in Kaposi sarcoma-associated herpesvirus infection and associated disease. Semin Immunopathol 42:143–157. https://doi.org/10.1007/s00281-020-00787-z
53. Jham BC, Ma T, Hu J, Chaisuparat R, Friedman ER, Pandolfi PP, Schneider A, Sodhi A, Montaner S. 2011. Amplification of the angiogenic signal through the activation of the TSC/mTOR/HIF axis by the KSHV vGPCR in Kaposi's sarcoma. PLoS One 6:e19103. https://doi.org/10.1371/journal.pone.0019103
54. Haque M, Kousoulas KG. 2013. The Kaposi's sarcoma-associated herpesvirus ORF34 protein binds to HIF-1α and causes its degradation via the proteasome pathway. J Virol 87:2164–2173. https://doi.org/10.1128/JVI.02460-12
55. Li Q, He M, Zhou F, Ye F, Gao S-J, Longnecker RM. 2014. Activation of Kaposi's sarcoma-associated herpesvirus (KSHV) by inhibitors of class III histone deacetylases: identification of sirtuin 1 as a regulator of the KSHV life cycle. J Virol 88:6355–6367. https://doi.org/10.1128/JVI.00219-14
56. Xie J, Ajibade AO, Ye F, Kuhne K, Gao SJ. 2008. Reactivation of Kaposi's sarcoma-associated herpesvirus from latency requires MEK/ERK, JNK and p38 multiple mitogen-activated protein kinase pathways. Virology 371:139–154. https://doi.org/10.1016/j.virol.2007.09.040
57. Wang SE, Wu FY, Chen H, Shamay M, Zheng Q, Hayward GS. 2004. Early activation of the Kaposi's sarcoma-associated herpesvirus RTA, RAP, and MTA promoters by the tetradecanoyl phorbol acetate-induced AP1 pathway. J Virol 78:4248–4267. https://doi.org/10.1128/JVI.78.8.4248-4267.2004
58. Arany Z, Huang LE, Eckner R, Bhattacharya S, Jiang C, Goldberg MA, Bunn HF, Livingston DM. 1996. An essential role for p300/CBP in the cellular response to hypoxia. Proc Natl Acad Sci U S A 93:12969–12973. https://doi.org/10.1073/pnas.93.23.12969
59. Carrero P, Okamoto K, Coumailleau P, O'Brien S, Tanaka H, Poellinger L. 2000. Redox-regulated recruitment of the transcriptional coactivators CREB-binding protein and SRC-1 to hypoxia-inducible factor 1alpha. Mol Cell Biol 20:402–415. https://doi.org/10.1128/MCB.20.1.402-415.2000
60. Dayan F, Roux D, Brahimi-Horn MC, Pouyssegur J, Mazure NM. 2006. The oxygen sensor factor-inhibiting hypoxia-inducible factor-1 controls expression of distinct genes through the bifunctional transcriptional character of hypoxia-inducible factor-1alpha. Cancer Res 66:3688–3698. https://doi.org/10.1158/0008-5472.CAN-05-4564
61. Hu C-J, Sataur A, Wang L, Chen H, Simon MC. 2007. The N-terminal transactivation domain confers target gene specificity of hypoxia-inducible factors HIF-1alpha and HIF-2alpha. Mol Biol Cell 18:4528–4542. https://doi.org/10.1091/mbc.e06-05-0419
62. Yu X, Shahir A-M, Sha J, Feng Z, Eapen B, Nithianantham S, Das B, Karn J, Weinberg A, Bissada NF, Ye F, Longnecker RM. 2014. Short-chain fatty acids from periodontal pathogens suppress histone deacetylases, EZH2, and SUV39H1 to promote Kaposi's sarcoma-associated herpesvirus replication. J Virol 88:4466–4479. https://doi.org/10.1128/JVI.03326-13
63. Chang J, Renne R, Dittmer D, Ganem D. 2000. Inflammatory cytokines and the reactivation of Kaposi's sarcoma-associated herpesvirus lytic replication. Virology 266:17–25. https://doi.org/10.1006/viro.1999.0077
64. Movafagh S, Crook S, Vo K. 2015. Regulation of hypoxia-inducible factor-1a by reactive oxygen species: new developments in an old debate. J Cell Biochem 116:696–703. https://doi.org/10.1002/jcb.25074
65. Sang N, Stiehl DP, Bohensky J, Leshchinsky I, Srinivas V, Caro J. 2003. MAPK signaling up-regulates the activity of hypoxia-inducible factors by its effects on p300. J Biol Chem 278:14013–14019. https://doi.org/10.1074/jbc.M209702200
66. Peyssonnaux C, Zinkernagel AS, Schuepbach RA, Rankin E, Vaulont S, Haase VH, Nizet V, Johnson RS. 2007. Regulation of iron homeostasis by the hypoxia-inducible transcription factors (HIFs). J Clin Invest 117:1926–1932. https://doi.org/10.1172/JCI31370
67. Viollet C, Davis DA, Tekeste SS, Reczko M, Ziegelbauer JM, Pezzella F, Ragoussis J, Yarchoan R, Lieberman PM. 2017. RNA sequencing reveals that Kaposi sarcoma-associated herpesvirus infection mimics hypoxia gene expression signature. PLoS Pathog 13:e1006143. https://doi.org/10.1371/journal.ppat.1006143